

# SCIENTIFIC REPORTS



OPEN

## Sustained acceleration of soil carbon decomposition observed in a 6-year warming experiment in a warm-temperate forest in southern Japan

Munemasa Teramoto<sup>1</sup>, Naishen Liang<sup>1</sup>, Masahiro Takagi<sup>2</sup>, Jiye Zeng<sup>1</sup> & John Grace<sup>3</sup>

To examine global warming's effect on soil organic carbon (SOC) decomposition in Asian monsoon forests, we conducted a soil warming experiment with a multichannel automated chamber system in a 55-year-old warm-temperate evergreen broadleaved forest in southern Japan. We established three treatments: control chambers for total soil respiration, trenched chambers for heterotrophic respiration ( $R_h$ ), and warmed trenched chambers to examine warming effect on  $R_h$ . The soil was warmed with an infrared heater above each chamber to increase soil temperature at 5 cm depth by about 2.5 °C. The warming treatment lasted from January 2009 to the end of 2014. The annual warming effect on  $R_h$  (an increase per °C) ranged from 7.1 to 17.8% °C<sup>-1</sup>. Although the warming effect varied among the years, it averaged 9.4% °C<sup>-1</sup> over 6 years, which was close to the value of 10.1 to 10.9% °C<sup>-1</sup> that we calculated using the annual temperature–efflux response model of Lloyd and Taylor. The interannual warming effect was positively related to the total precipitation in the summer period, indicating that summer precipitation and the resulting soil moisture level also strongly influenced the soil warming effect in this forest.

Soil respiration ( $R_s$ ) consists of root respiration (autotrophic respiration) and heterotrophic respiration ( $R_h$ ) by soil-dwelling microbiota, and it is the second largest carbon flux in terrestrial ecosystems. The global  $R_s$  was estimated at  $98 \pm 12$  GtC in 2008<sup>1</sup>, and  $R_h$  was estimated to be 57.1 GtC<sup>2</sup>, more than half of  $R_s$ .

Enzymatic activity by the soil microbiota is expected to increase with temperature, and previous studies have expressed the temperature sensitivity of  $R_h$  by using a simple exponential function<sup>3</sup>,  $Q_{10}$ , or other, more exact functions<sup>4,5</sup>. Many modelling studies have attempted to represent changes in the carbon cycle under global warming using a constant value of  $Q_{10}$ <sup>6–9</sup>. However, a recent study by Todd-Brown *et al.*<sup>10</sup> used several CMIP5 Earth System Models and showed that  $Q_{10}$  values for global soil carbon decomposition rates ranged from 1.45 to 2.61. The exponential function for  $Q_{10}$  implies that global  $R_h$  will rise dramatically with even a small increase in global temperatures. According to the worst-case RCP 8.5 scenario in the 5th IPCC report<sup>11</sup>, the world's temperature may increase by 2.6 to 4.8 °C by the end of the 21st century. Even though the global terrestrial ecosystem is now estimated to represent a carbon sink of  $2.4 \pm 0.7$  GtC<sup>12</sup>, rising temperatures are likely to convert much of this carbon sink into a carbon source due to the increased  $R_h$  that will occur under global warming<sup>13</sup>.

On the other hand, some studies have shown no evidence of a long-term exponential increase of soil CO<sub>2</sub> emission in response to global warming<sup>14–17</sup>. The decreased or weaker-than-expected soil warming effects can be explained by several factors, including differences in the quantity of soil organic carbon (SOC)<sup>18,19</sup>, precipitation and soil moisture<sup>20</sup>, thermal adaptation of microbiota due to shifts in enzymatic activity<sup>21</sup>, and changes in the microbial species composition<sup>22–24</sup> and biomass<sup>25</sup>.

<sup>1</sup>Center for Global Environmental Research, National Institute for Environmental Studies, Tsukuba, Ibaraki 305-8506, Japan. <sup>2</sup>Faculty of Agriculture, University of Miyazaki, 11300 Tano-cho, Miyazaki 889-1702, Japan. <sup>3</sup>Institute of Ecology and Resource Management, University of Edinburgh, Edinburgh EH9 3JU, UK. Correspondence and requests for materials should be addressed to N.L. (email: liang@nies.go.jp)

Using models with several soil carbon pools, previous studies have explained the decreased stimulatory effect of soil warming by rapid depletion of labile carbon fractions<sup>18,19</sup>. However, the temperature sensitivity of non-labile organic carbon fractions is also a serious concern for determining the long-term response of  $R_h$  to warming<sup>19,26</sup>. Therefore, the quantity of SOC appears to be critical for determining the long-term response of  $R_h$  to warming.

Stimulation of  $R_h$  by soil warming is also closely related to precipitation and soil moisture because soil warming tends to decrease the soil moisture content<sup>27</sup>. Water deficits decrease  $R_h$  and  $Q_{10}$  by suppressing microbial activity through the inhibition of solute diffusion and a decrease of substrate availability<sup>28,29</sup>. Thus, under water-deficit conditions, soil moisture could become the primary factor that will govern soil carbon decomposition, and the soil warming effect might not be apparent or might even suppress  $CO_2$  emission due to drying of the soil<sup>20,30</sup>.

To understand the long-term response of  $R_h$  to warming and the factors that affect the response, it is necessary to use long-term experiments. Recently, observations over long periods have begun to appear<sup>16,17,31–34</sup>, but the observed long-term warming effect has been inconsistent. More observations and interpretations are therefore urgently needed.

In the present work, we focused on a warm-temperate forest in southern Japan, where the monsoon climate is humid, drought is infrequent, and the soil is relatively rich in carbon<sup>35–37</sup>. To examine the trend of stimulatory soil warming effect on  $R_h$  under these humid and SOC-abundant conditions, and to analyse how the effects of interactions among various factors affected the response, we conducted a soil warming experiment. Most previous soil warming experiments were conducted in grasslands<sup>15,38,39</sup>, boreal coniferous forests<sup>16,18,40</sup>, and cool-temperate forests<sup>17,33,41</sup>. Our study therefore complements this previous research by providing new data about the long-term soil warming effect in a warm-temperate forest.

We used a multichannel, automated chamber measurement system to collect soil  $CO_2$  efflux data continuously under an artificially warmed environment in a warm-temperate evergreen broad-leaved forest site on Kyushu, in southern Japan. Continuous observation with a high-resolution dataset made it possible to detect the influences of short-term environmental changes on the soil  $CO_2$  efflux, thereby providing data suitable for accurate estimation of a potential long-term warming effect. This is important, because soil warming experiments with such continuous observations have been rare in the world warmer region. To our knowledge, this is the first experiment that examined the effect of soil warming on  $R_h$  using long-term continuous measurements in a warm-temperate forest.

## Results

**Soil carbon and nitrogen.** The SOC and total nitrogen (TN) contents in the upper 30 cm of the soil near chambers were averaged  $9.92 \pm 0.48 \text{ kg m}^{-2}$  and  $0.69 \pm 0.03 \text{ kg m}^{-2}$ , respectively. The C:N ratio of the upper 30 cm of the soil was 14.2. The SOC in the upper 5 cm was estimated to be  $2.23 \text{ kg m}^{-2}$  in trenched treatment ( $R_h$ ), and  $2.09 \text{ kg m}^{-2}$  in warmed trenched treatment ( $R_{hw}$ ) after 6 years of warming treatment in the end of December 2014. No significant warming effect on SOC content was confirmed.

**Seasonal variability of the  $CO_2$  flux and the influence of soil temperature and moisture.** We obtained 6 years of continuous soil  $CO_2$  efflux data ( $F_c$ ).  $F_c$  increased with increasing soil temperature in all treatments (Fig. 1a,b). The mean  $F_c$  values during the whole study period were  $4.13 \pm 0.36 \mu\text{mol CO}_2 \text{ m}^{-2} \text{ s}^{-1}$  for  $R_s$ ,  $3.14 \pm 0.08 \mu\text{mol CO}_2 \text{ m}^{-2} \text{ s}^{-1}$  for  $R_h$ , and  $3.63 \pm 0.16 \mu\text{mol CO}_2 \text{ m}^{-2} \text{ s}^{-1}$  for  $R_{hw}$ . The difference in efflux between  $R_{hw}$  and  $R_h$  usually peaked during the summer (July to September), but it decreased or even became negative when the soil moisture level was low during the summer or at the end of the spring (from late May to early June, Fig. 1c). During the whole measurement period,  $R_h$  accounted for 76.0% of  $R_s$ .

The estimated total annual carbon flux was  $15.7 \pm 1.4 \text{ tC ha}^{-1}$  for  $R_s$  (with a range from 13.4 to  $18.4 \text{ tC ha}^{-1}$  during the study period),  $11.9 \pm 0.3 \text{ tC ha}^{-1}$  for  $R_h$  (ranging from 10.3 to  $13.3 \text{ tC ha}^{-1}$ ), and  $13.8 \pm 0.6 \text{ tC ha}^{-1}$  for  $R_{hw}$  (ranging from 12.0 to  $15.1 \text{ tC ha}^{-1}$ ). The estimated carbon flux  $R_{hw}$  increased significantly due to the warming treatment both annually ( $p = 0.033$ ) and seasonally (during the dormant period,  $p = 0.028$ ) compared with  $R_h$ , but the difference was not significant during the growing period (from May to October) or the summer. Figure 2 shows the seasonal relationships between the estimated  $F_c$  and the soil temperature (Fig. 2a–c) and the soil moisture (Fig. 2d–f). This analysis revealed significant relationships between soil temperature and  $F_c$  in the dormant period ( $p < 0.050$ ,  $R^2 > 0.7$ , Fig. 2c). There was no significant relationship between soil temperature and each carbon flux in the summer, when the temperature range was relatively small (Fig. 2b). On the other hand, the relationship between soil moisture and  $F_c$  was only significant for  $R_{hw}$  during the summer ( $p = 0.013$ ,  $R^2 = 0.95$ , Fig. 2e). There was no relationship between soil moisture and  $F_c$  in the dormant period in all treatments (Fig. 2f).

**Temperature response of  $F_c$ .**  $F_c$  increased exponentially with increasing soil temperature in both the control and the warming treatment in all years ( $p < 0.0001$ ,  $R^2 > 0.80$ , Fig. 3a,b), with the exception of 2013 (for which the relationship was significant, but weaker, with  $R^2 > 0.70$ ).

**Response of  $F_c$  to soil moisture.** We analysed the relationship between  $F_c$  and soil moisture from July to September using temperature-normalized  $F_c$  ( $RF_c$ : the residuals of measured  $F_c$  and predicted values of  $F_c$  using Equation 4) (Fig. 4a,b). Usually, the relationship was a concave-down curve (i.e., exhibited a maximum value). However, the relationship was relatively weak when we used  $RF_c$  data from all 6 years ( $p < 0.0001$ ,  $R^2 = 0.23$  for  $R_s$ , 0.28 for  $R_h$ , 0.48 for  $R_{hw}$ , Fig. 4a,b). There was no significant relationship between  $RF_c$  and soil moisture in the summer of 2012 for  $R_s$  and  $R_h$ . However, we detected a moderately strong relationship in 2013 ( $p < 0.0001$ ,  $R^2 = 0.65$  for  $R_s$ , 0.58 for  $R_h$ , 0.56 for  $R_{hw}$ , Fig. 4a,b) when summer precipitation was the lowest in 6 years.

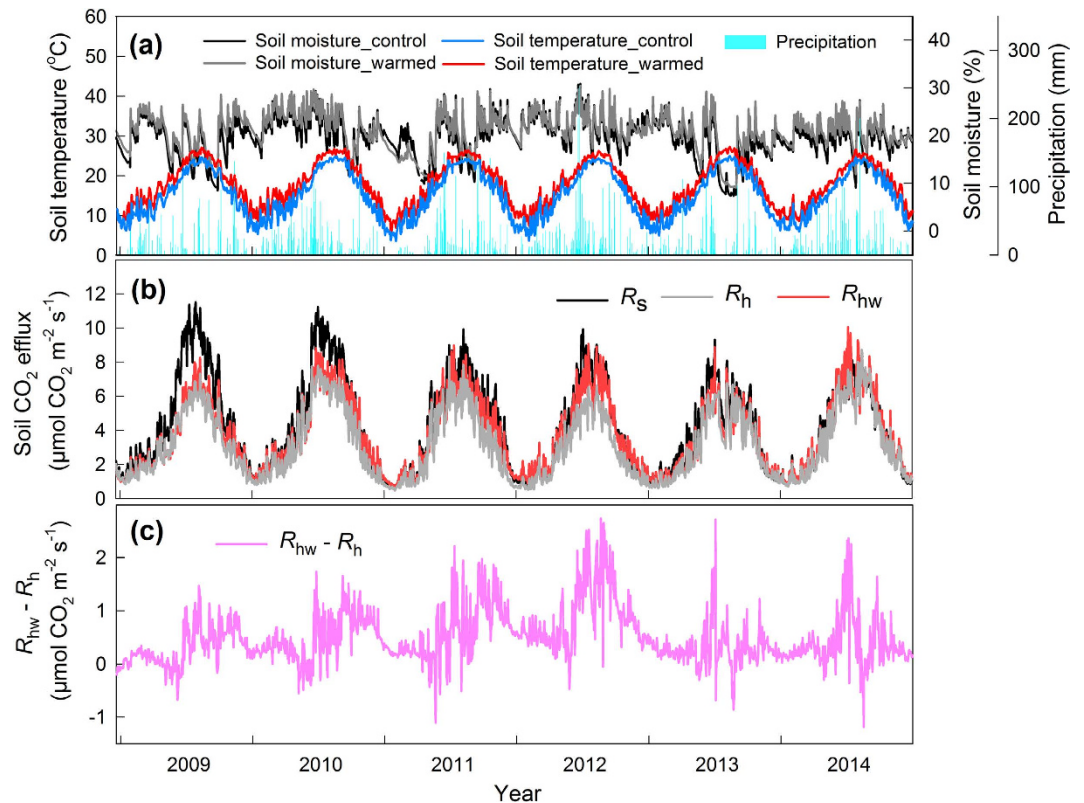


**Figure 1.** The seasonal changes of (a) soil temperature (at a depth of 5 cm) and soil moisture content (at a depth of 10 cm), (b) soil CO<sub>2</sub> efflux ( $R_s$ , soil respiration;  $R_{hw}$  and  $R_h$ , heterotrophic respiration in the warmed and control soil, respectively), and (c) the difference in efflux between the warmed and control treatments (i.e.,  $R_{hw} - R_h$ ).

**Temperature sensitivity of  $Q_{10}$ .** We analysed the temperature sensitivity of the carbon efflux ( $Q_{10}$ ). To remove the effect of soil moisture from this  $Q_{10}$  analysis, we filtered the  $F_c$  data to obtain values when soil moisture was within the range for the annual average of soil moisture  $\pm 1$  SD (i.e., the soil-moisture-normalized value). Figure 5a,b show the annual trends of  $Q_{10}$  values for the all measured data (raw- $Q_{10}$ ) and soil-moisture-normalized data (normalized- $Q_{10}$ ), respectively. The mean raw- $Q_{10}$  value for  $F_c$  was 2.73 (ranged from 2.34 to 2.97) for  $R_s$ , 2.65 (ranged from 2.36 to 2.90) for  $R_h$ , and 2.66 (ranged from 2.23 to 3.02) for  $R_{hw}$ . There was no significant difference in this overall average raw- $Q_{10}$  between  $R_h$  and  $R_{hw}$ . The decrease of raw- $Q_{10}$  in 2013 was remarkable in all treatments (Fig. 5a). On the other hand, we found that the normalized- $Q_{10}$  value increased to 3.00 (ranged from 2.83 to 3.10) for  $R_s$ , 2.88 (ranged from 2.69 to 3.24) for  $R_h$ , and 2.92 (ranged from 2.74 to 3.23) for  $R_{hw}$  (Fig. 5b). The annual normalized- $Q_{10}$  became more stable, and the decrease in the raw- $Q_{10}$  in 2013 disappeared. Similarly, there was no significant difference in the mean normalized- $Q_{10}$  between  $R_h$  and  $R_{hw}$ .

We found no significant relationship between the annual raw- $Q_{10}$  and soil temperature (Fig. 5c). However, we found marginally significant and significant negative relationships between soil temperature and the normalized- $Q_{10}$  for  $R_s$  ( $p = 0.081$ ,  $R^2 = 0.57$ ) and  $R_{hw}$  ( $p = 0.041$ ,  $R^2 = 0.69$ ), respectively (Fig. 5d). On the other hand, we found marginally significant concave-down relationships between summer soil moisture and the annual raw- $Q_{10}$  (Fig. 5e) for  $R_h$  ( $p = 0.070$ ,  $R^2 = 0.83$ ) and for  $R_{hw}$  ( $p = 0.071$ ,  $R^2 = 0.83$ ). In addition, we found significant and slightly stronger concave-down relationships between the total summer precipitation and the annual raw- $Q_{10}$  (Fig. 5f) for  $R_h$  ( $p = 0.018$ ,  $R^2 = 0.93$ ) and for  $R_{hw}$  ( $p = 0.031$ ,  $R^2 = 0.90$ ).

**Effect of warming on  $R_h$ .** Our measurements showed a clear seasonal pattern in the warming effect (Fig. 6). Overall, the warming effect increased from September to annual maximum peak in winter (from the middle of November to January), and decreased after the peak. The warming effect was kept low level from May to August. During the 6 years of measurement, the maximum peak of the warming effect was in early January 2012, and the effect decreased thereafter. We calculated modelled warming effect using raw- $Q_{10}$  model and normalized- $Q_{10}$  model. The modelled warming effect showed the same basic seasonal pattern: large in winter and small in summer (Fig. 6).

The annual warming effect was 7.1% °C<sup>-1</sup> in 2009, 8.1% °C<sup>-1</sup> in 2010, 10.8% °C<sup>-1</sup> in 2011, 17.8% °C<sup>-1</sup> in 2012, 7.2% °C<sup>-1</sup> in 2013, and 8.0% °C<sup>-1</sup> in 2014 (Fig. 7a). The annual variation in the warming effect was obvious, and the measured warming effect peaked in 2012, as shown in Fig. 6. However, the overall average warming effect for the study period was 9.4% °C<sup>-1</sup>, which is very close to the modelled warming effects (10.1% °C<sup>-1</sup> for the raw- $Q_{10}$  model, 10.9% °C<sup>-1</sup> for the normalized- $Q_{10}$  model). The interannual variation of the modelled warming effect

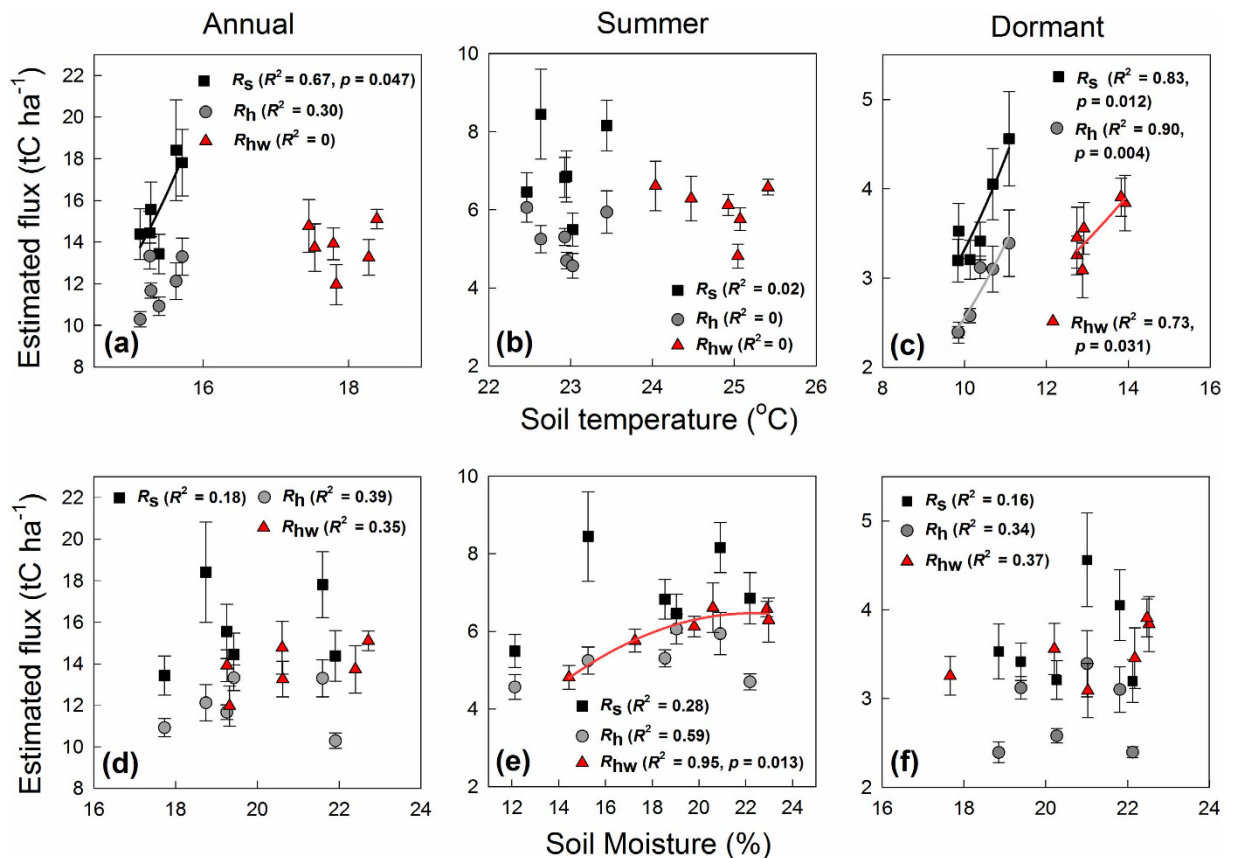


**Figure 2.** Relationships between the estimated  $F_c$  values ( $R_S$ , soil respiration;  $R_{hw}$  and  $R_h$ , heterotrophic respiration in the warmed and control soil, respectively) and the (a,b,c) average soil temperature at a depth of 5 cm and (d,e,f) soil moisture content at a depth of 10 cm for the (a,d) annual period, (b,e) summer, and (c,f) dormant period. ‘Summer’ means from July to September and ‘dormant period’ means from January to April and November to December of each year. Values are means  $\pm$  SEM.

was much smaller than that of the measured effect, ranging from 8.8 to 11.0%  $^{\circ}\text{C}^{-1}$  in the raw- $Q_{10}$  model and from 10.2 to 11.4%  $^{\circ}\text{C}^{-1}$  in the normalized- $Q_{10}$  version. The difference between the two versions of the modelled warming effect was biggest in 2013 (2.4%  $^{\circ}\text{C}^{-1}$ ), but was minor in the other years (0.1–1.2%  $^{\circ}\text{C}^{-1}$ ) as was shown in Figs 6 and 7a. There was no significant relationship between the annual warming effect and the annual mean soil temperature (Fig. 7b). On the other hand, we found a marginally significant positive relationship between the annual warming effect and the total summer precipitation ( $p = 0.085$ ,  $R^2 = 0.56$ , Fig. 7c).

## Discussion

The stimulatory effect of soil warming was maintained in all years, with no indication of any decrease or disappearance of the warming effect. Even though we observed strong interannual variation of the soil warming effect, its overall average value was 9.4%  $^{\circ}\text{C}^{-1}$ , which is very close to the values estimated by the traditional temperature response model. Regarding the magnitude of the soil warming effect on  $R_h$ , Wang *et al.*<sup>42</sup> estimated values of 13.5, 3.5, and 10.5%  $^{\circ}\text{C}^{-1}$  for forest, grassland, and an overall mean of 50 ecosystems (after 1 to 19 years of warming), and suggested that no apparent thermal adaptation had occurred after 4 years of warming. Our result agrees well with their report.

The sustainability of the warming effect in the present study appears to depend on the abundance of SOC. The amount of SOC (to a depth of 30 cm) at our study site (9.92 kg  $\text{m}^{-2}$ ) was slightly larger than the estimated average SOC for Japanese forest soils (9.0 kg  $\text{m}^{-2}$ )<sup>35</sup>, which in turn was 1.7 times the world average. From this perspective, the SOC content was high at our forest site. Some authors have explained a decreasing trend for the warming effect after several years of warming by hypothesizing depletion of the labile C pools<sup>18,19</sup>. Indeed, in a warming experiment that used the same protocol with our study conducted in a mixed-forest in an old-peatland in northern Japan with abundant SOC, the warming effect remained as high as 26%  $^{\circ}\text{C}^{-1}$  during four growing seasons, which is even more remarkable than the present results<sup>33</sup>. In our research site, no significant influence of soil warming treatment on SOC was confirmed. However, it is possible that a period of 6 years might be not enough to confirm the significant warming effect on SOC. Further continuous warming treatment with temporal analysis of SOC will be needed to accurately examine the long-term warming effect on SOC. In addition, not only the quantitative dynamics of SOC under warming, we should also note the soil warming effect on the SOC

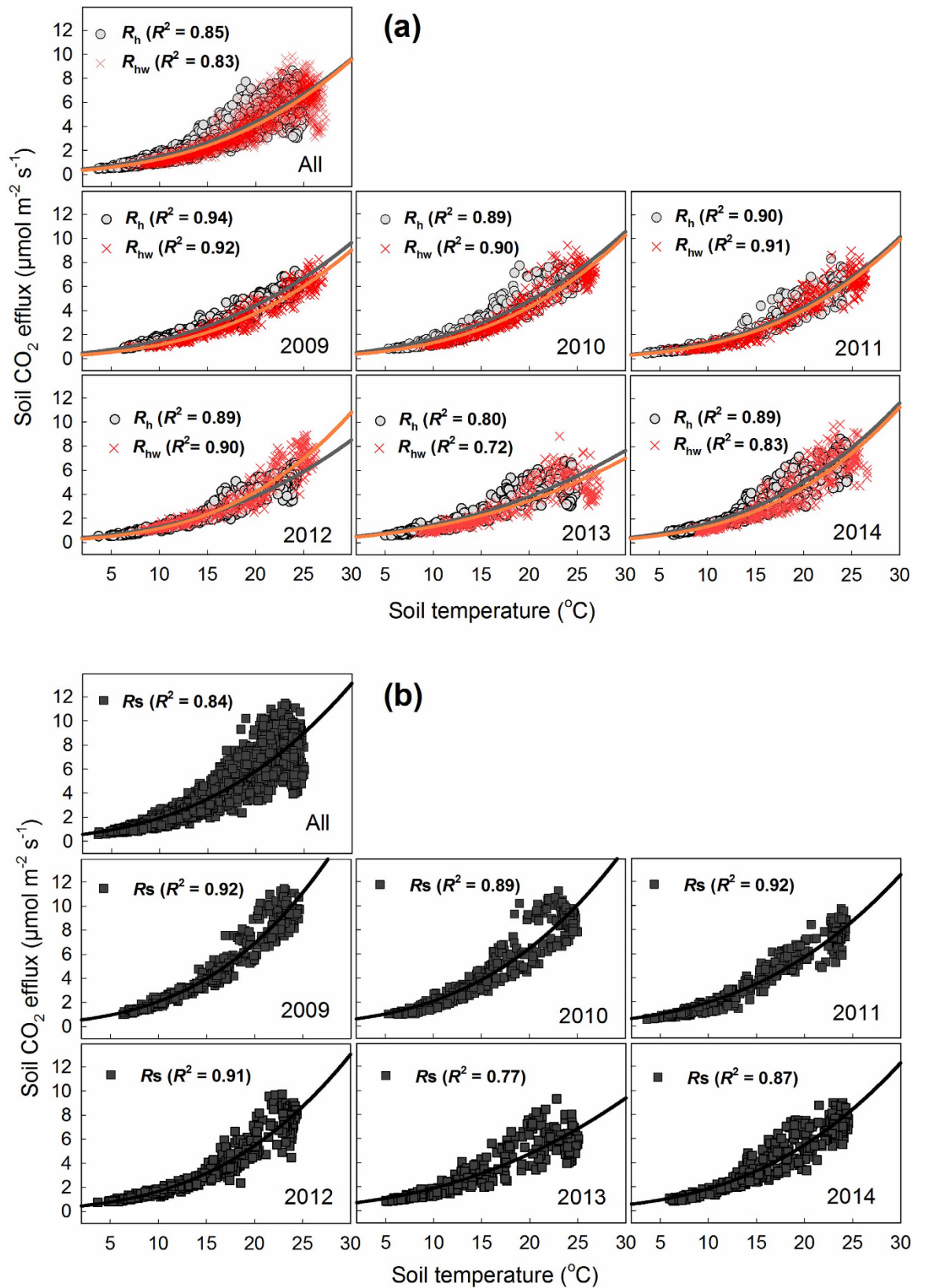


**Figure 3.** Temperature response of soil CO<sub>2</sub> efflux for (a) heterotrophic respiration in the control ( $R_h$ ) and warmed ( $R_{hw}$ ) treatments and (b) soil respiration ( $R_s$ ) in each year. Soil temperature was measured at a depth of 5 cm. Regression lines are only presented for statistically significant relationships ( $p < 0.0001$ ). The equation of Lloyd and Taylor (Equation 4) was used for the fitted curve.

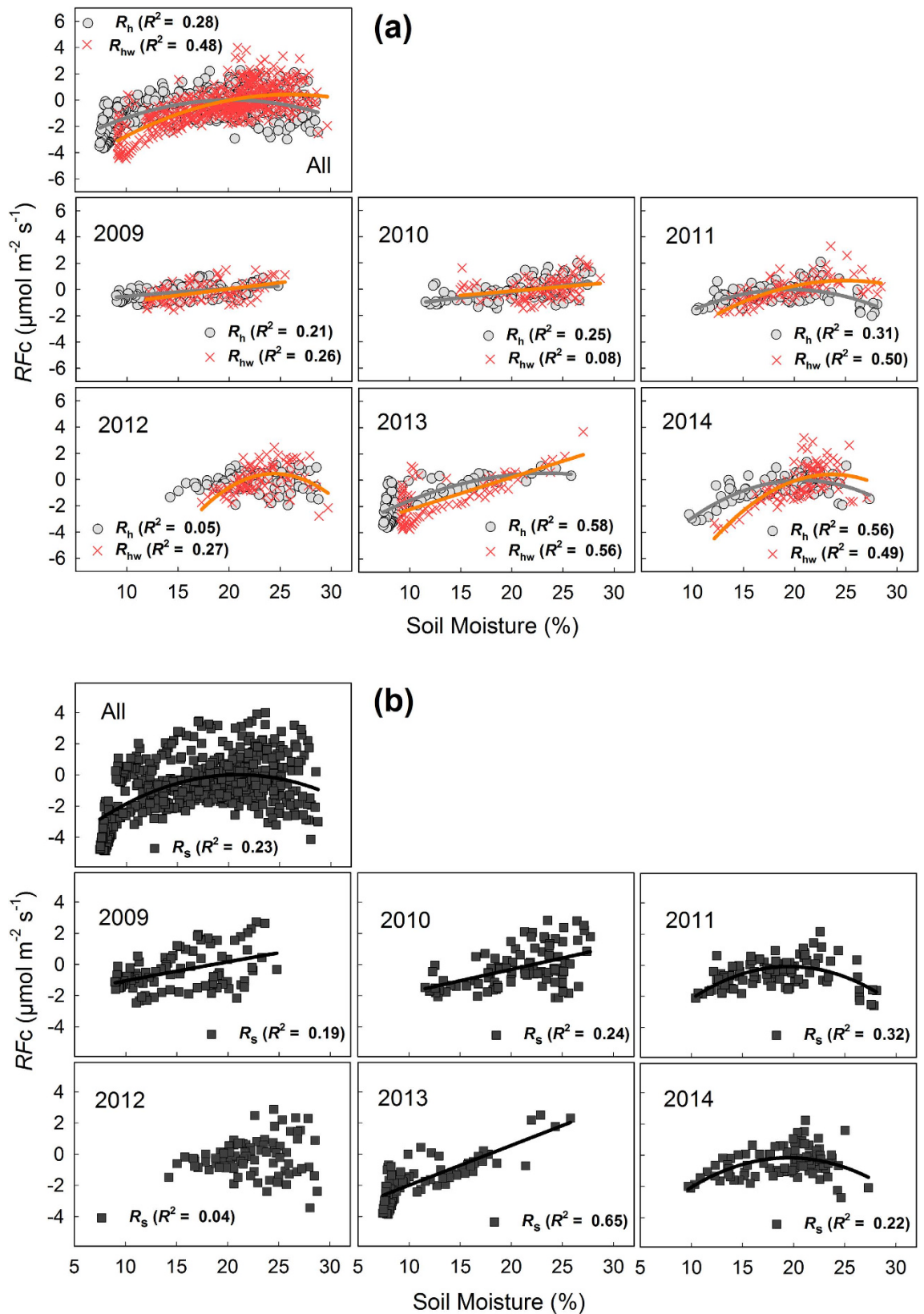


**Figure 4.** Moisture response of the temperature-normalized  $F_c$  ( $RF_c$ ) from the fitted curves in Figure for (a) heterotrophic respiration in the control ( $R_h$ ) and warmed treatment ( $R_{hw}$ ) and (b) soil respiration ( $R_s$ ) from July to September in each year. Regression lines are only presented for statistically significant relationships ( $p < 0.01$ ). Soil moisture content was measured at a depth of 10 cm.

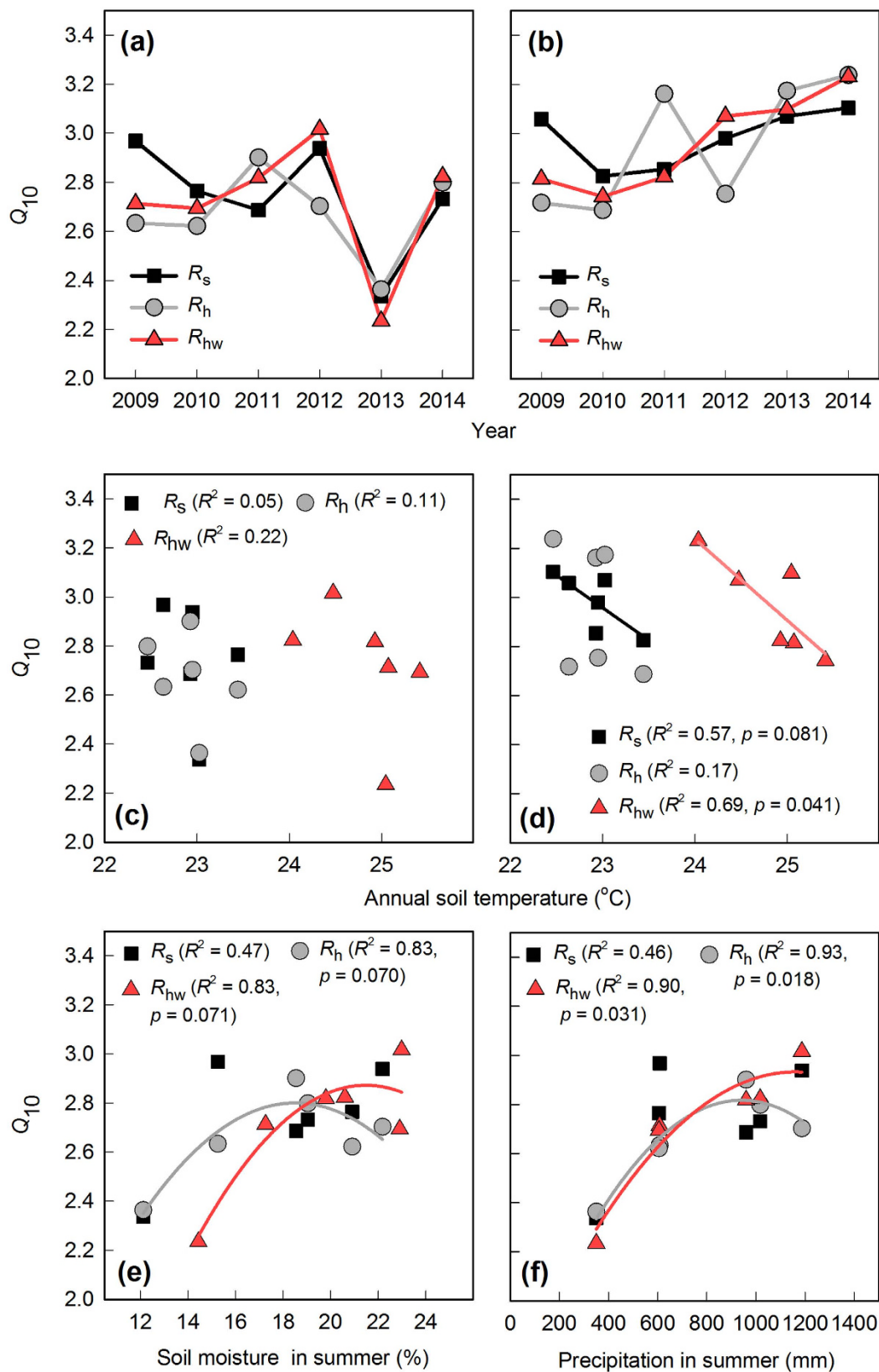


**Figure 5.** Annual trends of (a)  $Q_{10}$  (raw- $Q_{10}$ ) and (b) soil-moisture-normalized  $Q_{10}$  (normalized- $Q_{10}$ ). Relationships between the mean annual temperature and (c) raw- $Q_{10}$  and (d) normalized- $Q_{10}$ . Relationships between (e) soil moisture in the summer (from July to September) and raw- $Q_{10}$  and between (f) precipitation in summer and raw- $Q_{10}$ . The normalized- $Q_{10}$  was calculated from  $F_c$  data only when the soil moisture content was within the range of annual average  $\pm 1$  SD. Regression lines are only presented for statistically significant relationships ( $p < 0.1$ ).

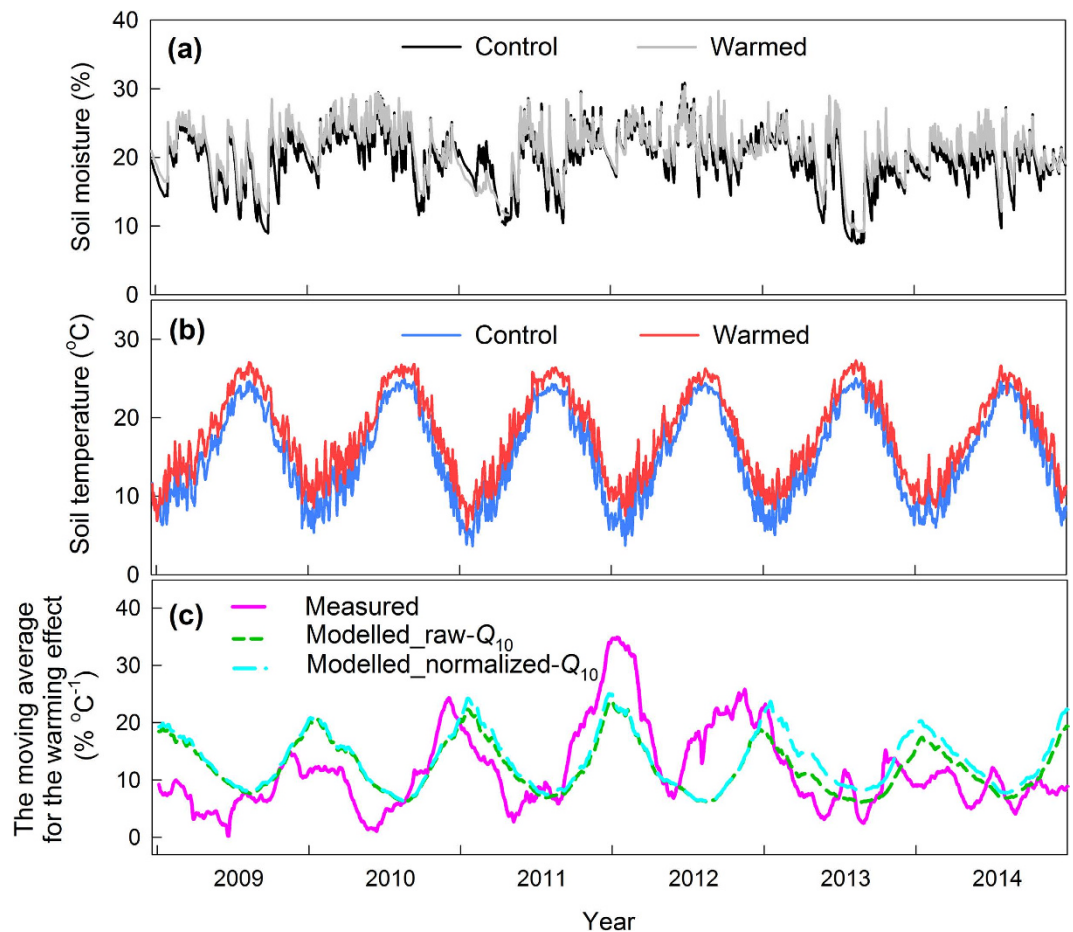


**Figure 6.** Seasonal variation of (a) soil moisture content, (b) soil temperature, and (c) the 31-day moving average for the warming effect. Raw- $Q_{10}$  model values were estimated from the annual temperature-response equation of Lloyd and Taylor (Equation 4) using the all measured data without accounting for soil moisture anomalies. Normalized- $Q_{10}$  model values were estimated from the equation that only included  $F_c$  data from times when the soil moisture was within the range of annual average  $\pm 1$  SD.

decomposition processes by microbiota because previous studies<sup>22–24</sup> and our collaborative study (Kondo *et al. in preparation*) confirmed the shift of species composition of microbiota under soil warming.

The soil nitrogen content is also important for decomposition of organic carbon by the microbiota. Nitrogen and microbial biomass are positively correlated<sup>43</sup>, and decomposition of organic carbon will be difficult under nitrogen-limited conditions even if SOC is abundant. Concerning temperature sensitivity, it has been found that the  $Q_{10}$  of  $R_h$  was positively correlated with the nitrogen-to-carbon (N:C) ratio in soil<sup>44</sup>. This suggested that the  $Q_{10}$  of  $R_h$  is smaller under nitrogen-limited conditions. The nitrogen content to a depth of 30 cm at our research site was  $0.69 \text{ kg m}^{-2}$ , and the average C:N ratio was 14.2. The limit of nitrogen mineralization and immobilization is thought to occur at a C:N ratio of 20<sup>45</sup>. Below this threshold, nitrogen mineralization is thought to occur. Thus, the soil nitrogen content and C:N ratio at our research site do not appear to have been nitrogen limited, so the nitrogen content was not a limiting factor for  $R_h$ . These results suggest that the co-occurrence of abundant SOC and adequate nitrogen can explain why the stimulatory effect of soil warming was maintained throughout our study period.

At our forest site, we found a strong and marked exponential relationship between soil temperature and  $F_c$  in each year and in both the control and the warming treatment (Fig. 3a,b). In addition, the relationship between seasonally estimated  $F_c$  and soil temperature was strong, especially in dormant period (Fig. 2c). These results suggest that soil temperature is the primary environmental factor that controls the seasonal variation of  $F_c$ , as was shown by Lloyd and Taylor<sup>4</sup>.

$Q_{10}$  is reported to decrease with increasing temperature<sup>46,47</sup>. However, the  $Q_{10}$  of  $R_{hw}$  in our study did not differ significantly from that of  $R_h$ , and we found no decreasing trend for  $Q_{10}$  after 6 years of the warming treatment. This result indicates that the thermal adaptation of temperature sensitivity did not occur. Schindlbacher *et al.*<sup>41</sup> also showed that  $Q_{10}$  did not decrease after 9 years of warming treatment in a soil incubation experiment, and suggested that no thermal adaptation of  $R_h$  should be expected after long-term soil warming. We found no significant relationship between the mean annual soil temperature and raw- $Q_{10}$ , but found a significant negative relationship between the normalized- $Q_{10}$  and the mean annual soil temperature for  $R_{hw}$ . This indicates that the



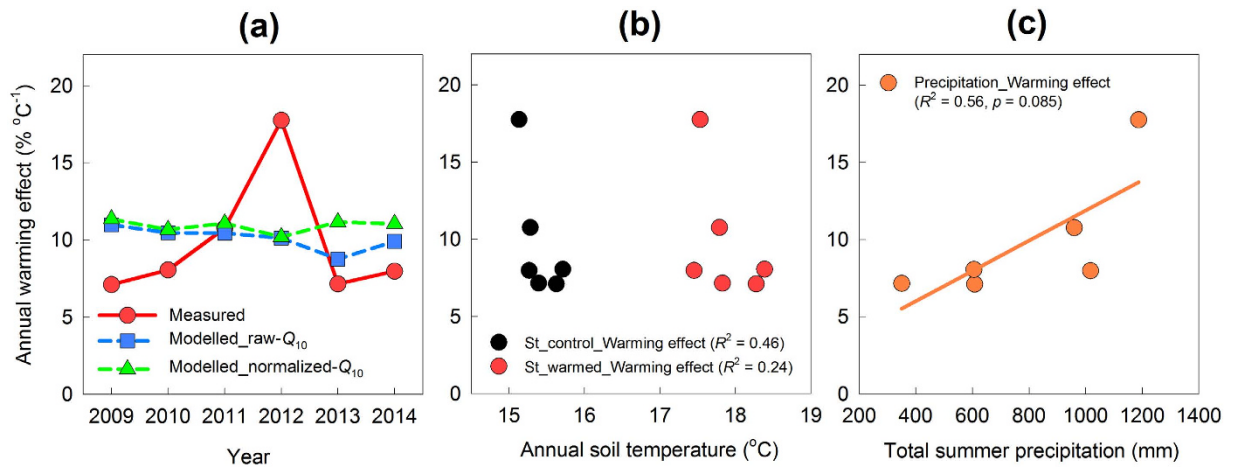


**Figure 7.** (a) Annual variation in the warming effect on soil CO<sub>2</sub> efflux (measured values, and values estimated using the raw-Q<sub>10</sub> model and the normalized-Q<sub>10</sub> model). (b) Relationships between the mean annual soil temperature (control and warmed) and the annual warming effect. (c) Relationships between the total summer precipitation (from July to September) and the annual warming effect. Regression lines are only shown for statistically significant relationships ( $p < 0.1$ ).

influence of the summer soil moisture on the interannual variation of  $Q_{10}$  is stronger than that of the mean annual soil temperature. However, it is difficult to confirm the direct influence of the mean annual soil temperature on the interannual variation of  $Q_{10}$  because of the small interannual variation of soil temperature (15.1 to 15.7 °C in the control, versus 17.5 to 18.4 °C in the warming treatment). The result only partly implies that an increase in the mean annual soil temperature could cause  $Q_{10}$  to decrease under a warmer climate.

According to the temperature-response model of Lloyd and Taylor<sup>4</sup>, the stimulatory effect of soil warming on soil  $F_c$  should decrease with increasing temperature. In our study, the seasonal trend of the warming effect peaked in the winter and decreased in the summer, and the simulated warming effect calculated from Lloyd and Taylor's model showed the same seasonal trend. On the other hand, we found no significant relationship between the annual warming effect and the annual soil temperature. This may be because of the weak relationship between the mean annual soil temperature and the interannual variation of raw-Q<sub>10</sub>, which represents a stronger influence of soil moisture during the summer and a narrow range of annual soil temperatures. From these perspectives, the influence of soil temperature on the seasonal trend of the warming effect was clear, but the interannual pattern was more difficult to explain.

Overall, the relationship between soil moisture and  $F_c$  during the summer was not strong. However, that relationship was strong in all treatments in 2013 due to the low summer rainfall that year. When we considered the influence of soil moisture on the interannual trend for  $F_c$ , we found a significant relationship between the estimated summer  $F_c$  and the seasonal mean soil moisture content for  $R_{hw}$ . These results suggest that the influence of soil moisture on the seasonal variation of  $F_c$  was unclear, except during the summer drought, but that the influence was clear for the interannual variation of  $F_c$ , especially for  $R_{hw}$ . The warming treatment did not change the annual mean soil moisture content significantly at a depth of 10 cm, but the strong relationship between the estimated summer  $F_c$  and the seasonal mean soil moisture content for  $R_{hw}$  implies that the demand for water was relatively strong in the top 10 cm of the warmed soil.

Both the seasonal mean soil moisture content and the total summer precipitation were significantly related to raw-Q<sub>10</sub> for  $R_h$  and  $R_{hw}$ . The peak raw-Q<sub>10</sub> for  $R_h$  was in 2011 (2.90). The soil moisture content and precipitation in that summer were 18.5% and 960 mm, respectively. Higher soil moisture content and precipitation led to a slight decrease in raw-Q<sub>10</sub>. A concave-down relationship between soil moisture content and the  $Q_{10}$  of  $R_h$  was shown in a previous study<sup>28</sup>. On the other hand, the peak raw-Q<sub>10</sub> for  $R_{hw}$  was in 2012 (3.02), the year with the most precipitation (1187.5 mm). The raw-Q<sub>10</sub> for  $R_{hw}$  in response to summer precipitation increased with high precipitation in summer, and did not show the decreasing trend along with the increase of summer precipitation (Fig. 5f). An increasing trend with increasing soil moisture was confirmed for  $Q_{10}$  of  $R_s$  in relatively arid environments<sup>48,49</sup>. This suggests that the difference in trends depends on whether the water supply available to support  $F_c$  was sufficient for the soil microbiota. From this perspective, the response of annual  $Q_{10}$  to summer precipitation can differ between  $R_h$  and  $R_{hw}$ , and suggests higher water demand under soil warming than in the control during the summer. The estimated summer  $F_c$  values account for about 45% of the estimated annual values in each treatment at our forest site. Precipitation and the resulting increase in soil moisture content appear to strongly influence the annual temperature sensitivity by affecting the trend in summer  $F_c$ .

We found a marginally significant relationship between the total summer precipitation and the annual soil warming effect. The different responses of the temperature sensitivity of  $R_h$  and  $R_{hw}$  to summer precipitation and the resulting change in soil moisture content appear to contribute to the annual variation in the warming effect. In addition, we found wide ranges of seasonal variation in total summer precipitation and soil moisture content. The summer precipitation ranged from 350.5 to 1187.5 mm during our study. The mean summer soil moisture content

ranged from 12.1 to 22.2% in the control treatment and from 14.4 to 23.0% in the warming treatment. These wide ranges from dry to moist explain some of the annual variation in the warming effect.

There has been no information in the literature on the long-term effect of soil warming on  $R_h$  in warm-temperate forests. Using a multichannel automated chamber measurement system and infrared heater for warming the soil, we provide the first evidence that the stimulatory effect of soil warming on soil  $R_h$  is maintained for at least 6 years, and the magnitude of the effect was comparable to values predicted using a traditional temperature-response model. In addition, we found that the interannual variation in effect of soil warming on  $R_h$  was positively related to the total summer precipitation. Overall, our results suggest that the stimulatory effect of soil warming in an Asian monsoon forest with abundant SOC and a humid climate may be maintained for a longer period than was previously expected. Under the predicted future warmer and more humid conditions, the carbon sink strength of these forests will therefore potentially be weakened as a result of increased  $R_h$ . Of course, the photosynthetic uptake of carbon by the trees may also increase, thereby balancing the soil carbon loss to some unknown extent. We will need further continuous  $F_c$  measurements to support a decade-level estimation and determine whether the results of the present study remain valid over longer time periods. In addition, it is necessary to conduct long-term warming experiments at other forest sites with a variety of soils to confirm how widely the present results can be generalized.

## Materials and Methods

**Site description.** The study site is in a warm-temperate evergreen broad-leaved forest in the Miyazaki University Forest (31°51'N, 131°18'E; 130 m asl), Kyushu, southern Japan. The dominant species is *Castanopsis cuspidata* and *Machilus thunbergii* (about 55 years old). The forest's understory was dominated by *Eurya japonica*. The tree density is about 1175 stems ha<sup>-1</sup>. We used climate records (2009 to 2014) from the Japan Meteorology Agency weather observation station in Miyazaki as reference data. The mean annual temperature was 17.6 °C, with monthly means ranging from 7.0 °C in January to 27.9 °C in August, and the mean annual precipitation was 2604 mm, with 70% of the total occurring during the growing season. The soil is a well-drained brown forest soil developed from volcanoclastic sediment, and the thicknesses of the A and B horizons were 20 and 40 cm, respectively. Soil pH in the upper 40 cm averaged 5.7, mildly acidic as commonly observed in Japanese forest soil.

**Chamber system.** To obtain continuous soil CO<sub>2</sub> flux measurements, we used a multichannel automated chamber system. The system was a modified version of the system described by Liang *et al.*<sup>50,51</sup>. The main components of this system were an infrared gas analyser (IRGA; LI-820, Li-Cor, Lincoln, NE, USA), a datalogger (CR1000, Campbell Scientific Inc., Logan, UT, USA), an air compressor (super oil-free BEBICON 0.2 LP-7s, Hitachi Ltd., Tokyo, Japan) and handmade 15 chambers. Square chambers (90 cm long × 90 cm wide × 50 cm tall) were made of a plastic-coated steel frame (30 mm × 30 mm) to which was affixed a clear PVC wall. They were connected to the control box with a power supply, thermocouples for measurement of air and soil temperatures (5 cm below the soil surface), and tubing for sampling and circulating the air. Thermocouples from these chambers were connected to the handmade multiplexer, and signals were output to the CR1000 datalogger. Soil moisture sensors (CS616, Campbell Scientific Inc.) were buried 10 cm below the soil surface within the chambers, and their signals were also recorded by the data logger. Each chamber was also connected to the compressed air for opening and closing of the chamber lid via an electric valve and two pneumatic cylinders (LAC-20B, CKD Corp., Nagoya, Japan) attached to the lid of each chamber. This enabled continuous and automatic opening and closing according to a program installed in the data logger. Only one chamber was closed at a time, during a flux measurement period that lasted for 4 min, then was re-opened after the measurement to allow measurement of the next chamber. By repeating this cycle, measurements in all chambers were completed within an hour. During each measurement, two embedded electric fans (MF12B, Nihon Blower Ltd., Tokyo, Japan) stirred the air inside the closed chamber to even out the CO<sub>2</sub> concentration. Air inside the closed chamber was then passed through the IRGA in the control box with a micro-diaphragm pump (5.0 L min<sup>-1</sup>; CM-50, Enomoto Ltd., Tokyo, Japan). The data logger recorded signals from the IRGA and other sensors at 10-s intervals.

The system was first installed in December 2008. Before starting the warming treatment in January 2009, we established trenches around 10 of the 15 chambers to keep out roots, and then carefully clipped all understory vegetation growing inside the chamber thus excluding root respiration and letting us measure heterotrophic respiration ( $R_h$ ). During this operation, a root-cutting chainsaw was used to sever any roots in the soil to a depth of 40 cm. PVC plates (100 × 30 × 0.4 cm) were then inserted around each trenched chamber to prevent roots from growing into the chamber. Soil CO<sub>2</sub> efflux ( $F_c$ , μmol CO<sub>2</sub> m<sup>-2</sup> s<sup>-1</sup>) was measured for 19 days after the trenching treatment to measure  $R_h$  in those trenched 10 chambers before warming treatment. Thereafter, a warming treatment was set up for five of the trenched chambers (the other five were the control treatment). For the warming treatment, an infrared heater (Carbon lump heater, Sakaguchi E.H. VOC corp., Tokyo, Japan) was hung at the centre of each warmed chamber ( $R_{hw}$ ), about 1.6 m above the soil surface. Due to this warming treatment, soil temperature at a depth of 5 cm below the surface increased by about 2.5 °C above the soil temperature of control treatment. The trenching treatment was not applied to five additional chambers, which we used to measure total soil respiration ( $R_s$  = the sum of heterotrophic and autotrophic respiration).

**Data processing and analysis.**  $F_c$  was calculated with the following equation:

$$F_c = \frac{VP}{RST} \frac{\delta C}{\delta t} \quad (1)$$

where,  $V$  is the chamber volume ( $\text{m}^3$ ),  $P$  is the air pressure (Pa),  $R$  is the ideal gas constant ( $8.314 \text{ Pa m}^3 \text{ K}^{-1} \text{ mol}^{-1}$ ),  $S$  is the soil surface area inside the chamber ( $\text{m}^2$ ),  $T$  is the air temperature (K) inside the chamber, and  $\delta C/\delta t$  is the rate of change of the  $\text{CO}_2$  mole fraction ( $\mu\text{mol mol}^{-1} \text{ s}^{-1}$ ) calculated from the chamber data using the least-squares method and based on the assumption of a linear change during the measurement period. Before we calculated the average  $F_c$  in each treatment, we applied the Smirnov–Grubbs test (with significance at  $p < 0.1$ ) for the average of  $F_c$  values during the 6 years for all chambers in each experimental group to remove outlier data that showed an unusual  $F_c$  pattern from the analysis.

To analyse the temperature response of each chamber and treatment, we used regression analysis following an exponential model:

$$F_c = ae^{bT_s} \quad (2)$$

where  $a$  is the efflux at  $0^\circ\text{C}$ ,  $b$  is a curve-fitting parameter for temperature sensitivity, and  $T_s$  is the soil temperature ( $^\circ\text{C}$ ). From Equation (2),  $Q_{10}$  can be calculated to express the increase in soil respiration for every  $10^\circ\text{C}$  temperature rise, as follows:

$$Q_{10} = e^{10b} \quad (3)$$

where  $b$  is the curve-fitting parameter from Equation 2. We used this equation to derive a mean value of  $Q_{10}$  from the annual temperature response curve of  $F_c$ . In addition, we also calculated the soil-moisture-normalized  $Q_{10}$  values using  $F_c$  data when the soil moisture content was within the range of variation in the soil moisture (annual average  $\pm 1$  SD; hereafter, normalized- $Q_{10}$ ). To examine the influence of warming on annual  $Q_{10}$ , we used the two-tailed Student's  $t$ -test for the relationship between  $R_h$  and  $R_{hw}$  (with significance at  $p < 0.05$ ).

On the other hand, Lloyd and Taylor<sup>4</sup> developed the following model to represent  $F_c$ :

$$F_c = R_{\text{ref}} e^{E_0 \left( \frac{1}{T_{\text{ref}} - T_0} - \frac{1}{T_s - T_0} \right)} \quad (4)$$

where  $R_{\text{ref}}$  ( $\mu\text{mol CO}_2 \text{ m}^{-2} \text{ s}^{-1}$ ) is the soil  $\text{CO}_2$  efflux at a specified reference soil temperature,  $E_0$  is the coefficient of temperature sensitivity,  $T_{\text{ref}}$  is the specified reference soil temperature ( $288.15 \text{ K}$ ),  $T_0$  is the soil temperature when  $R_s$  is zero ( $227.13 \text{ K}$ ), and  $T_s$  is the observed soil temperature (K). We used this Equation (4) in our study to fill gaps in the data and when we ran the annual temperature-response equation of  $F_c$ .

The number of gap days totalled 105 days during the 2202 days of measurement from December 2008 to December 2014, corresponding to 4.8% of the whole measurement period. The biggest gap was from 29 September to 31 October 2013 due to problem of the IRGA, and this was the only gap longer than 30 days during the 6 years of observations. We analysed the temperature-response of  $F_c$  for each chamber in every year. We used Equations (2) and (3) to calculate the  $Q_{10}$  values, and Equation (4) to estimate  $F_c$  for data gaps in each chamber. After the gap-filling, the estimated annual or seasonal fluxes ( $\text{tC ha}^{-1}$ ) were calculated for three seasons: the summer, from July to September; the growing period, from May to October; and the dormant period, from January to April and from November to December. To examine the influence of warming on the estimated fluxes, we performed the two-tailed Student's  $t$ -test on the 6-year average value for each period to test for differences between  $R_h$  and  $R_{hw}$  (with significance at  $p < 0.05$ ).

To avoid the confounding effects of soil temperature and soil moisture, we first subtracted the predicted values of  $F_c$  using Equation (4) from the observed values, and the resulting residual values (the temperature-normalized  $F_c$ ) were used to analyse the relationships between soil moisture and  $F_c$ . To calculate the strength of the relationship, we used the following quadratic regression:

$$RF_c = a_1\theta^2 + a_2\theta + a_3 \quad (a_1 > 0) \quad (5)$$

where  $RF_c$  ( $\mu\text{mol CO}_2 \text{ m}^{-2} \text{ s}^{-1}$ ) means the temperature-normalized  $F_c$ ,  $\theta$  is the volumetric soil moisture content (%),  $a_1$ ,  $a_2$ , and  $a_3$  are curve-fitting parameters. However, when the value of  $a_1$  in Equation (5) was 0 or negative, we used Equation (6) instead:

$$RF_c = a_1\theta + a_2 \quad (6)$$

We used SigmaPlot 12.5 (Systat Software, San Jose, CA, USA) as our statistical software for our analyses.

**Analysis of the warming effect.** To analyse the warming effect on  $R_h$ , we first calculated treatment coefficients for  $R_h$  and  $R_{hw}$  based on 18 days of hourly  $F_c$  data from each chamber from 20 December 2008 to 6 January 2009 to modify the heterogeneity of the  $F_c$  value between  $R_h$  and  $R_{hw}$  before the start of the warming treatment in January 2009. We calculated the coefficients as  $F_{c(\text{all})}/F_{c(\text{treatment})}$ , where  $F_{c(\text{all})}$  means the average of the hourly  $F_c$  in the trenched chambers ( $\mu\text{mol CO}_2 \text{ m}^{-2} \text{ s}^{-1}$ ) during the 18 days before the warming treatment began, and  $F_{c(\text{treatment})}$  represents the average hourly  $F_c$  for each treatment during the same period ( $R_h$  or  $R_{hw}$ ,  $\mu\text{mol CO}_2 \text{ m}^{-2} \text{ s}^{-1}$ ). Those coefficients were calculated to be 0.9665 for  $R_h$  and 1.0359 for  $R_{hw}$ , respectively. Thus, the warming effect on  $F_c$  ( $\% \text{ } ^\circ\text{C}^{-1}$ ) was calculated as  $(1.0359 R_{hw} - 0.9665 R_h) \times 100 / [0.9665 R_h (T_{sw} - T_{sc})]$ , where  $T_{sc}$  is the soil temperature in the  $R_h$  treatment ( $^\circ\text{C}$ ), and  $T_{sw}$  is the soil temperature in the  $R_{hw}$  treatment ( $^\circ\text{C}$ ). Modelled  $F_c$  values for  $R_h$  and  $R_{hw}$  were calculated by assigning the soil temperatures in the  $R_h$  and  $R_{hw}$  treatments to the annual temperature-response equation for  $R_h$  (Equation 4). There were two versions of the modelled  $F_c$ : the 'raw- $Q_{10}$ ' version (in which we used the all measured data without accounting for soil moisture anomalies) and the 'normalized- $Q_{10}$ ' version. For the normalized- $Q_{10}$  version, the annual temperature-response equation using Equation (4) for  $R_h$  was derived from the same range of soil moisture values that we used when calculating

the normalized- $Q_{10}$ . Then, the modelled warming effect ( $\% \text{ } ^\circ\text{C}^{-1}$ ) was calculated for the two versions of the model as  $(R_{h-T_{sw}} - R_{h-T_{sc}}) \times 100 / [R_{h-T_{sc}} (T_{sw} - T_{sc})]$ , where  $R_{h-T_{sc}}$  is the modelled  $F_c$  of  $R_h$  ( $\mu\text{mol CO}_2 \text{ m}^{-2} \text{ s}^{-1}$ ) and  $R_{h-T_{sw}}$  is the modelled  $F_c$  of  $R_{hw}$  ( $\mu\text{mol CO}_2 \text{ m}^{-2} \text{ s}^{-1}$ ) calculated by substituting soil temperature in  $R_{hw}$  to annual temperature-response equation of  $R_h$ . We calculated the 31-day moving averages (from 15 days before to 15 days after a given date) from the observed daily warming effect and the two versions of the model. We also calculated the observed and modelled annual warming effects from the annual average of daily  $F_c$ .

**Analysis of soil carbon and nitrogen.** To analyse the soil organic carbon (SOC) and total nitrogen (TN) concentrations, we hammered three PVC tubes (10.7 cm in inner-diameter, 70 cm in length) into the soil to obtain samples to a depth of 30 cm in June 2014, about 1–2 m from three of the chambers. The soil cores were cut into six 5-cm segments for analysis, and those soil samples were dried in a  $80^\circ\text{C}$  oven for 1 week. After weighting the dried soil samples, each segment was passed through a 2-mm sieve to remove coarse fragments and large roots. The dried soil samples were then ground into a fine powder with a mortar and further dried at  $100^\circ\text{C}$  for 1 week. The SOC and TN contents were analysed using an NC analyser (FLASH EA 1112, Thermo Electron Corp., Waltham, MA, USA) with combustion at  $900^\circ\text{C}$ . In the middle of August 2016, we also sampled small soil cores (5.0 cm in diameter) to a depth of 5 cm in three of the trenched and the warmed trenched chambers to examine the warming effect on SOC (warming treatment was still continued until that time). We performed small soil core sampling in that way to minimize soil disturbance in each chamber due to soil core sampling. The SOC contents in those small soil cores were analysed following the same procedure as the above. Difference in SOC between control and warming treatments was corrected on the assumption that SOC decreased lineally along with time due to soil warming treatment (from the start of warming treatment, early January in 2009) to estimate SOC content in warmed soil in the end of December 2014. We performed the two-tailed Student's  $t$ -test on SOC content in each treatment to examine if there was significant effect of soil warming on SOC (with significance at  $p < 0.05$ ).

## References

- Bond-Lamberty, B. & Thomson, A. Temperature-associated increases in the global soil respiration record. *Nature* **464**, 579–U132, doi: 10.1038/nature08930 (2010).
- Potter, C. S. & Klooster, S. A. Interannual variability in soil trace gas ( $\text{CO}_2$ ,  $\text{N}_2\text{O}$ , NO) fluxes and analysis of controllers on regional to global scales. *Global Biogeochem. Cycles* **12**, 621–635, doi: 10.1029/98GB02425 (1998).
- Xu, M. & Qi, Y. Spatial and seasonal variations of  $Q_{10}$  determined by soil respiration measurements at a Sierra Nevada forest. *Global Biogeochem. Cycles* **15**, 687–696, doi: 10.1029/2000gb001365 (2001).
- Lloyd, J. & Taylor, J. A. On the temperature dependence of soil respiration. *Funct. Ecol.* **8**, 315–323, doi: 10.2307/2389824 (1994).
- Davidson, E. A. & Janssens, I. A. Temperature sensitivity of soil carbon decomposition and feedbacks to climate change. *Nature* **440**, 165–173, doi: 10.1038/nature04514 (2006).
- Jenkinson, D. S., Adams, D. E. & Wild, A. Model estimates of  $\text{CO}_2$  emissions from soil in response to global warming. *Nature* **351**, 304–306, doi: 10.1038/351304a0 (1991).
- Raich, J. W. *et al.* Potential net primary productivity in south America: application of a global model. *Ecol. Appl.* **1**, 399–429, doi: 10.2307/1941899 (1991).
- Potter, C. S. *et al.* Terrestrial ecosystem production: a process model based on global satellite and surface data. *Global Biogeochem. Cycles* **7**, 811–841, doi: 10.1029/93GB02725 (1993).
- Cox, P. M., Betts, R. A., Jones, C. D., Spall, S. A. & Totterdell, I. J. Acceleration of global warming due to carbon-cycle feedbacks in a coupled climate model. *Nature* **408**, 184–187, doi: 10.1038/35041539 (2000).
- Todd-Brown, K. E. O. *et al.* Causes of variation in soil carbon simulations from CMIP5 Earth system models and comparison with observations. *Biogeosciences* **10**, 1717–1736, doi: 10.5194/bg-10-1717-2013 (2013).
- IPCC. *Climate Change 2013: The Physical Science Basis. Contribution of Working Group I to the Fifth Assessment Report of the Intergovernmental Panel on Climate Change.* (Cambridge University Press, 2013).
- Sitch, S. *et al.* Recent trends and drivers of regional sources and sinks of carbon dioxide. *Biogeosciences* **12**, 653–679, doi: 10.5194/bg-12-653-2015 (2015).
- Friedlingstein, P. *et al.* Climate-carbon cycle feedback analysis: results from the C<sup>4</sup>MIP model intercomparison. *J. Clim.* **19**, 3337–3353, doi: 10.1175/JCLI3800.1 (2006).
- Grace, J. & Rayment, M. Respiration in the balance. *Nature* **404**, 819–820, doi: 10.1038/35009170 (2000).
- Luo, Y. Q., Wan, S. Q., Hui, D. F. & Wallace, L. L. Acclimatization of soil respiration to warming in a tall grass prairie. *Nature* **413**, 622–625, doi: 10.1038/35098065 (2001).
- Strömgren, M. Soil-surface  $\text{CO}_2$  flux and growth in a boreal Norway Spruce stand. Effects of soil warming and nutrition. *Unpublished PhD, Swedish University of Agricultural Sciences, Uppsala*, 220 pp (2001).
- Melillo, J. M. *et al.* Soil warming and carbon-cycle feedbacks to the climate system. *Science* **298**, 2173–2176, doi: 10.1126/science.1074153 (2002).
- Eliasson, P. E. *et al.* The response of heterotrophic  $\text{CO}_2$  flux to soil warming. *Global Change Biol.* **11**, 167–181, doi: 10.1111/j.1365-2486.2004.00878.x (2005).
- Knorr, W., Prentice, I. C., House, J. I. & Holland, E. A. Long-term sensitivity of soil carbon turnover to warming. *Nature* **433**, 298–301, doi: 10.1038/nature03226 (2005).
- Schindlbacher, A. *et al.* Soil respiration under climate change: prolonged summer drought offsets soil warming effects. *Global Change Biol.* **18**, 2270–2279, doi: 10.1111/j.1365-2486.2012.02696.x (2012).
- Allison, S. D., Wallenstein, M. D. & Bradford, M. A. Soil-carbon response to warming dependent on microbial physiology. *Nat. Geosci.* **3**, 336–340, doi: 10.1038/ngeo846 (2010).
- Zogg, G. P. *et al.* Compositional and functional shifts in microbial communities due to soil warming. *Soil Sci. Soc. Am. J.* **61**, 475–481, doi: 10.2136/sssaj1997.03615995006100020015x (1997).
- Xiong, J. B. *et al.* Characterizing changes in soil bacterial community structure in response to short-term warming. *FEMS Microbiol. Ecol.* **89**, 281–292, doi: 10.1111/1574-6941.12289 (2014).
- Creamer, C. A. *et al.* Microbial community structure mediates response of soil C decomposition to litter addition and warming. *Soil Biol. Biochem.* **80**, 175–188, doi: 10.1016/j.soilbio.2014.10.008 (2015).
- Bradford, M. A. *et al.* Thermal adaptation of soil microbial respiration to elevated temperature. *Ecol. Lett.* **11**, 1316–1327, doi: 10.1111/j.1461-0248.2008.01251.x (2008).
- Kirschbaum, M. U. F. Soil respiration under prolonged soil warming: are rate reductions caused by acclimation or substrate loss? *Global Change Biol.* **10**, 1870–1877, doi: 10.1111/j.1365-2486.2004.00852.x (2004).

27. Xu, W. *et al.* A meta-analysis of the response of soil moisture to experimental warming. *Environ. Res. Lett.* **8**, doi: 10.1088/1748-9326/8/4/044027 (2013).
28. Craine, J. M. & Gelderman, T. M. Soil moisture controls on temperature sensitivity of soil organic carbon decomposition for a mesic grassland. *Soil Biol. Biochem.* **43**, 455–457, doi: 10.1016/j.soilbio.2010.10.011 (2011).
29. Moyano, F. E., Manzoni, S. & Chenu, C. Responses of soil heterotrophic respiration to moisture availability: an exploration of processes and models. *Soil Biol. Biochem.* **59**, 72–85, doi: 10.1016/j.soilbio.2013.01.002 (2013).
30. Suseela, V., Conant, R. T., Wallenstein, M. D. & Dukes, J. S. Effects of soil moisture on the temperature sensitivity of heterotrophic respiration vary seasonally in an old-field climate change experiment. *Global Change Biol.* **18**, 336–348, doi: 10.1111/j.1365-2486.2011.02516.x (2012).
31. Reth, S., Graf, W., Reichstein, M. & Munch, J. C. Sustained stimulation of soil respiration after 10 years of experimental warming. *Environ. Res. Lett.* **4**, doi: 10.1088/1748-9326/4/2/024005 (2009).
32. Lamb, E. G. *et al.* A high arctic soil ecosystem resists long-term environmental manipulations. *Global Change Biol.* **17**, 3187–3194, doi: 10.1111/j.1365-2486.2011.02431.x (2011).
33. Aguilos, M. *et al.* Sustained large stimulation of soil heterotrophic respiration rate and its temperature sensitivity by soil warming in a cool-temperate forested peatland. *Tellus B* **65**, doi: 10.3402/tellusb.v65i0.20792 (2013).
34. Wu, C. *et al.* Heterotrophic respiration does not acclimate to continuous warming in a subtropical forest. *Sci. Rep.* **6**, 21561, doi: 10.1038/srep21561 (2016).
35. Morisada, K., Ono, K. & Kanomata, H. Organic carbon stock in forest soils in Japan. *Geoderma* **119**, 21–32, doi: 10.1016/S0016-7061(03)00220-9 (2004).
36. Water resources Department of the Ministry of Land, Infrastructure, Transport and Tourism, Japan. Water in Japan [http://www.mlit.go.jp/mizukokudo/mizsei/mizukokudo\\_mizsei\\_tk2\\_000008.html](http://www.mlit.go.jp/mizukokudo/mizsei/mizukokudo_mizsei_tk2_000008.html) (2014).
37. FAO (Food and Agriculture Organization of the United Nations). *Aquastat* <http://www.fao.org/nr/water/aquastat/main/index.stm> (2013).
38. Hartley, I. P., Heinemeyer, A. & Ineson, P. Effects of three years of soil warming and shading on the rate of soil respiration: substrate availability and not thermal acclimation mediates observed response. *Global Change Biol.* **13**, 1761–1770, doi: 10.1111/j.1365-2486.2007.01373.x (2007).
39. Niu, S. L., Sherry, R. A., Zhou, X. H. & Luo, Y. Q. Ecosystem carbon fluxes in response to warming and clipping in a tallgrass prairie. *Ecosystems* **16**, 948–961, doi: 10.1007/s10021-013-9661-4 (2013).
40. Bronson, D. R., Gower, S. T., Tanner, M., Linder, S. & Van Herk, I. Response of soil surface CO<sub>2</sub> flux in a boreal forest to ecosystem warming. *Global Change Biol.* **14**, 856–867, doi: 10.1111/j.1365-2486.2007.01508.x (2008).
41. Schindlbacher, A., Schnecker, J., Takriti, M., Borken, W. & Wanek, W. Microbial physiology and soil CO<sub>2</sub> efflux after 9 years of soil warming in a temperate forest - no indications for thermal adaptations. *Global Change Biol.* **21**, 4265–4277, doi: 10.1111/gcb.12996 (2015).
42. Wang, X. *et al.* Soil respiration under climate warming: differential response of heterotrophic and autotrophic respiration. *Global Change Biol.* **20**, 3229–3237, doi: 10.1111/gcb.12620 (2014).
43. Hartman, W. H. & Richardson, C. J. Differential nutrient limitation of soil microbial biomass and metabolic quotients ( $qCO_2$ ): is there a biological stoichiometry of soil microbes? *PLoS One* **8**, e57127, doi: 10.1371/journal.pone.0057127 (2013).
44. He, N. & Yu, G. Stoichiometrical regulation of soil organic matter decomposition and its temperature sensitivity. *Ecol. Evol.* **6**, 620–627, doi: 10.1002/ece3.1927 (2016).
45. Tate, R. L. *Soil microbiology* (John Wiley & Sons, Inc., 1995).
46. Kirschbaum, M. U. F. The temperature dependence of soil organic matter decomposition, and the effect of global warming on soil organic C storage. *Soil Biol. Biochem.* **27**, 753–760, doi: 10.1016/0038-0717(94)00242-s (1995).
47. Kirschbaum, M. U. F. Will changes in soil organic carbon act as a positive or negative feedback on global warming? *Biogeochemistry* **48**, 21–51, doi: 10.1023/a:1006238902976 (2000).
48. Wang, W., Peng, S. S., Wang, T. & Fang, J. Y. Winter soil CO<sub>2</sub> efflux and its contribution to annual soil respiration in different ecosystems of a forest-steppe ecotone, north China. *Soil Biol. Biochem.* **42**, 451–458, doi: 10.1016/j.soilbio.2009.11.028 (2010).
49. Wang, B. *et al.* Soil moisture modifies the response of soil respiration to temperature in a desert shrub ecosystem. *Biogeosciences* **11**, 259–268, doi: 10.5194/bg-11-259-2014 (2014).
50. Liang, N., Inoue, G. & Fujinuma, Y. A multichannel automated chamber system for continuous measurement of forest soil CO<sub>2</sub> efflux. *Tree Physiol.* **23**, 825–832, doi: 10.1093/treephys/23.12.825 (2003).
51. Liang, N., Hirano, T., Zheng, Z. M., Tang, J. & Fujinuma, Y. Soil CO<sub>2</sub> efflux of a larch forest in northern Japan. *Biogeosciences* **7**, 3447–3457, doi: 10.5194/bg-7-3447-2010 (2010).

## Acknowledgements

We thank to Dr. Toshiaki Kondo in Hiroshima University for providing data concerning DNA analysis of soil microbiota. This research was financially supported by the Global Environment Research Fund (B-073) and the Global Environment Research Account for National Institutes (Evaluation of the potential effect of global warming on soil carbon emission of Japanese forest ecosystems) of the Ministry of the Environment Government of Japan. This study was also partially supported by the NIES Internal Call for Research Proposals (A) of 2014 (Evaluation of soil CO<sub>2</sub> efflux of Asian forest ecosystems based on an automated chamber network), the Japan Society for the Promotion of Science–China (Ministry of Science and Technology) International Collaboration Project of 2015 (Integrated evaluation of potential changes in both forest soil microbial biomass and compositions by using environmental DNA; no. 15032041-000127), and a Grant-in-Aid for Scientific Research (no. 22310019) from the Japanese Ministry of Education, Culture, Sports, Science and Technology.

## Author Contributions

N.L. designed the experiment and wrote the manuscript, M.T. analysed the data and wrote the manuscript, M.T. conducted the field experiment, J.Z. developed a computer program for analysing the data and J.G. wrote the manuscript.

## Additional Information

**Competing financial interests:** The authors declare no competing financial interests.

**How to cite this article:** Teramoto, M. *et al.* Sustained acceleration of soil carbon decomposition observed in a 6-year warming experiment in a warm-temperate forest in southern Japan. *Sci. Rep.* **6**, 35563; doi: 10.1038/srep35563 (2016).



This work is licensed under a Creative Commons Attribution 4.0 International License. The images or other third party material in this article are included in the article's Creative Commons license, unless indicated otherwise in the credit line; if the material is not included under the Creative Commons license, users will need to obtain permission from the license holder to reproduce the material. To view a copy of this license, visit <http://creativecommons.org/licenses/by/4.0/>

© The Author(s) 2016